Stony Brook University

Interrogation of possible imaging conditions for radiation sensitive metal organic frameworks in transmission electron microscopes

A Thesis Presented

by

Wei Yu Pan

to

The Graduate School

in Partial Fulfillment of the

Requirements

for the Degree of

Material of Science

in

Material Science and Engineering

Stony Brook University

May 2016

Stony Brook University

The Graduate School

Wei Yu Pan

We, the thesis committee for the above candidate for the

Master of Arts degree, hereby recommend

acceptance of this thesis.

Dr. Houlin Xin–Thesis Asvisor
Staff Scientist, Electron Microscopy Group
Center for Functional Nanomaterial(CFN)
Brookhaven National Laboratory

T. Venkatesh
Associate Professor, Graduate Program Director
Department of Materials Science and Engineering

Jon Sokolov
Professor
Department of Materials Science and Engineering

This thesis is accepted by the Graduate School

Charles Taber
Dean of the Graduate School

Abstract of the thesis

Interrogation of possible imaging conditions for radiation sensitive metal organic frameworks in transmission electron microscopes

by

Wei Yu Pan

Material of Science

in

Material Science and Engineering

Stony Brook University

2016

Although transmission electron microscopy (TEM) is extremely powerful at the characterization of materials on the nano- and atomic scales, the advantages introduce accompanying drawbacks. That is, high energy electrons offer the structural information while imparting radiation damage to the samples. Metal organic frameworks are a new class of materials that have potential applications in gas storage and catalysis. A direct imaging of their lattice structures is highly desired. However, these samples are extremely radiation sensitive. In order to characterize their structures, low-dose TEM need to be performed. To date, there is a lack of a

systematic of radiation study of the radiation sensitive of MOFs. To fill this gap, in this thesis we performed a systematically study of the critical dose of a series of metal organic framework (MOF) samples in TEM.

We characterized the critical dose for Cu, Ni, NiCu, NiCo, CoCu and NiCoCu MOFs samples using time lapsed electron diffraction measurement. We found that within our test range, the critical dose is independent of dose rate. We also found that the MOF the samples that contain nickel are more resistance to radiation damage. In contrast, the MOFs that contain copper are more radiation sensitive. For NiCo and CoCu MOFs, their critical dose are 999.18 ($\frac{e^-}{Å^2}$) and 28.41 ($\frac{e^-}{Å^2}$) respectively. By adding copper the NiCo MOF to form NiCuCo MOF, the critical dose is reduced from 999.18 ($\frac{e^-}{Å^2}$) to only 16.98 ($\frac{e^-}{Å^2}$), suggesting the copper can significantly affect the properties of the MOF structure. We also analyzed the diffraction pattern of MOFs attempting to build a correlation between the critical dose and maximal lattice spacing. However, we found that the maximum critical dose does not always track the maximal spacing. Through this research, we can calculate the suitable dose rate for either imaging or diffraction tomography measurement for these samples.

Keywords: TEM, Metal Organic Frameworks (MOFs), dose test, radiation damage, elastic and inelastic scattering, electron diffraction

Table of contents

List of figures

List of tables

List of abbreviations

TEM	Transmission Electron Microscopy
XEDS	X-ray Energy- Dispersive Spectrometry
EELS	Electron Energy-Loss Spectrometry
SEM	Scanning Electron Microscopy
STEM	Scanning Transmission Electron Microscopy
MOFs	Metal Organic Frameworks (MOFs)
CCS	Carbon Capture and Storage (CCS)
IL	Ionic liquids
RMIM	1-R-3-methylimidazolium
DR	Dose Rate
D	Electron Dose

Acknowledgment

I am extremely grateful to Dr. Houlin Xin for his guidance, support and training at Center for Functional Nanomaterial (CFN), Brookhaven National Laboratory (BNL)

I am thankful to [Professor Name] and [Professor Name] for their suggestions

I am thankful to all the department faculty and staff for their continuous supervision.

I also thank my parents, sister, colleagues and friends for their caring and support.

Chapter 1

Introduction

1.1 Radiation damage

A modern TEM is not only a tool fabricating high resolution image but also primarily a signal-generating and detecting instrument. Electrons beam radiated an area is a process of ionizing. Ionizing radiation produces secondary electrons analyzed by X-ray energy dispersive spectrometry (XEDS) and electron energy-loss spectrometry (EELS). However, it brings damage to the specimen.

1.1.1 Interaction between electrons and matters

Electrons, unlike X-ray, are charged so that it interact very strongly with matters and the wavelength of electrons can be controlled by potential. In general, wavelength of X-way is around 1-100Å, making it to probe structure much smaller than the size we can see in optical microscope. The wavelength of electrons can be shorter than X-ray by increasing potential based on the wave-particle duality proposed by De Broglie in 1924. These properties makes us can easily obtain the information from samples and acquires more information than X-ray.

Electrons interact strongly with atoms via Coulomb forces. Therefore, the thickness of specimen has to be very thin to allow electrons transmit. Based on

whether electrons conserve energy after colliding specimen, there are two types of scattering. One is elastic scattering (electron-nucleus scattering) that preserved beam energy and coherent (in step after collision with specimen), and, on the contrary, the other is inelastic scattering (electron-electron scattering). In TEM, elastic scattering play an important role in forming a diffraction pattern and an image on the screen. [1]

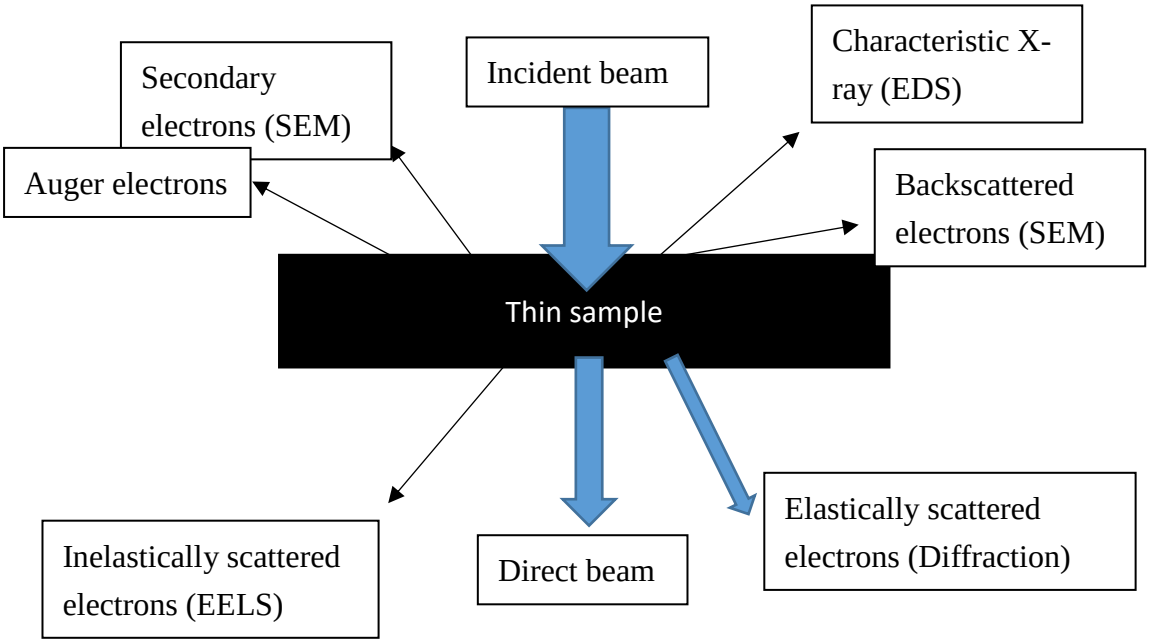

Figure 1. Interaction between electrons and thin sample

1.1.2 Interaction cross section and free mean path

To make accurate data, a single scattering event is ideal for TEM due to the more scattering event, the more complicated interpretation of the data. That's why finding the thinnest area or having thinner specimen is better in TEM. Thick samples enable multiple scattering, causing complicated calculations and less precise result.

Consequently, cross section, representing the chance that a scattering event will

occur, takes into account. So the larger cross section, the larger probability of scattering occurs. First, we consider across section for single atom.

$\sigma_{atom} = \pi r^2$, where r is the radius of atom

And then we move on to specimen with N atoms in volume of weight, that is, the cross section for a specimen will be

$\sigma_{total} = N\sigma_{atom}$

Note that the unit of σ_{atom} is m^{-1}, and N atoms in volume of weight can be replaced by $N = \frac{N_0 \rho}{A}$, where N_0 is Avogadro's number, A is atomic weight and ρ is density of atom.

Therefore, σ_{total} can be defined as the number of scattering events per unit length. If specimen has thickness t, cross section of specimen is given by

$\sigma_{total}\ t = N\sigma_{atom} t = \frac{N_0(\rho t)\,\sigma_{atom}}{A}$

, which display the thicker of specimen is, the higher probability of scattering will be.

Instead using cross section to interpret scattering, distance is more important because we can decide the thickness of specimen based on the distance "free mean path" (λ), an average distance between scattering events.

$$\lambda = \frac{1}{\sigma_{total}} = \frac{A}{N_0 \rho\, \sigma_{atom}}$$

In this thesis where accurately analyzing diffraction pattern and image is needed, making scattering as close to kinematical scattering as possible is ideal, therefore recording images from the thinnest area is required. As a result, cross section and free mean path do factor in the whole experiment. [2]

1.1.3 Radiation damage

Although inelastic collisions and elastic scatterings give us extraordinary useful signals to characterize the structure, the side effects they bring about are extraordinary catastrophic damage, which is called electron-beam damage or less precise called radiation damage. Electron beam can virtually damage every sample. Consequently, radiation damage has turned into be a limit in TEM research. Avoiding or minimizing radiation damage on MOFs samples is the primary purpose in this thesis. Totally, there are 3 types of elastic-caused damage and 4 types of inelastic-caused damage.

Before detailing types of radiation damage, we need to define some terminology. First, electron dose defined as the charge collide with limited area of specimen ($e^-/Å^2$), which can be transferred to electron exposure (C/m^2) due to $e = 1.6 * 10^{-19}$ C. In this thesis, we keep using $e^-/Å^2$ as unit of electron dose. The other terminology called critical dose (D_e) are defined as the dose where intensity decreased to $\frac{1}{e}$ = 37% of initial value. Critical dose is a value considered as electron-beam resistance of a material. The radiation sensitivity can be given based on critical dose as damage cross-section: $\sigma_d = e/D_e$, where e is electron charge.

1.1.4 Inelastic-caused damage

There are four types of inelastic-caused damage: radiolysis, heating, electrostatic

charging (same type in elastic-caused damage) and hydrocarbon contamination.

1.1.4.1 Radiolysis

Radiolysis is defined as chemicals degradation, break of chemical bond through inelastic scattering. This is the worst scenarios of electron-beam damage for polymers including organic and inorganic. After radiolysis, chemical bonds are broken and could turn side groups into reactive free radicals that could crosslink to from the other structure different from original one, resulting embarrassing misjudgement. If polymer specimen was crystalline initially, electron-beam damage result in loss of crystallinity which is observed as a diffused reflections, resulting in being amorphous structure. Alteration of electronic configuration causes a loss of fine structure in EELS spectrum, on the other hand, the bond breakage brings about mass loss. The majority mass loss are light atoms: hydrogen, oxygen particularly. The dose required for mass loss and composition change in organic specimen is higher than the dose that causes reflection fading (long-range order) but less than the dose resulting in loss of fine structure (short-range order). In this thesis, we only considered distorted long-range order, reflection fading. To investigate loss of fine structure, utilizing EELS is one of methods.

There are methods tackling the radiolysis

(1) Low dose imaging techniques

(2) Cool the specimen to liquid nitrogen temperature

(3) Coat the specimen with a conducting metal film.

(4) Use STEM imaging

(5) Minimize cross section of inelastic scattering by increasing the voltage of TEM

1.1.4.2 Heating

The vibrations of bonds will arise as result of phonons, and these are equivalent to heating specimen. The only way to reduce heating damage is to cool the specimen. This damage only need to be considered when specimen's thermal conduction is very low, ceramic particle for example. [3]

1.1.4.3 Hydrocarbon contamination

Different from knock-on damage that is loss of mass, hydrocarbon contamination is gain of mass. This effect occur when hydrocarbon molecules on the surface of specimen are polymerized by electron beam. Although vacuum and equipment are improved, specimen could be a source of hydrocarbons which can be removed by plasma cleaner before experiments.

1.1.5 Elastic-caused damage

There are three types of elastic-caused damage: atomic displacement, electron beam sputtering and electrostatic charging.

1.1.5.1 Atomic displacement or knock-on damage

Knock-on damage or displacement damage related to incident beam energy is a ubiquitous situation when electron beam hitting specimen. Elastic scattering means none of energy lose after interacting with nucleus. However, an electron that is scattered by a atomic nucleus (atomic mass A) must transfer energy E (unit in eV).

The amount of energy E can be presented as followed:

$E = E_{max}\{\sin(\frac{\theta}{2})\}^2$

$E_{max} = E_0(1.02 + \frac{E_0}{10^6})$ / 465.7A, where E_0 is the accelerating voltage (unit in eV)

If scattered angle θ is very small, scattered from outer or valence electron, the transfer energy E is very small, even could be negligible. However, if scattered angle is large (> 90^o or even = 180^o), this could cause atomic displacement if the energy exceed displacement energy (E_d), which is the same parameter we considered at knock-on damage. This damage causes decreasing in crystallinity.

The beam transfer its energy to knock out atoms in metal, resulting in formation of

vacancies, interstitials, or even dislocations. To knock out atoms, the beam electron need to penetrate close to nucleus and to be braked in its path, transferring almost all of its energy to atom. Also, the energy metal atoms bonding is also a critical parameter that is given by Hobbs.

$E_t = \frac{\sqrt{\frac{100+AE_d}{5}} - 10}{20}$ where threshold energy (E_t) in MeV and displacement energy (E_d) in eV. To avoid knock-on damage is to operate below threshold energy and to minimize electron dose.

Nickel-base alloy C-276 radiated by 300 keV electron beam has been found high density dislocation loops caused by atomic displacement, hardening the alloy. [4]

1.1.5.2 Electron sputtering

Electron sputtering is similar to atomic displacement, but different from atomic displacement, sputtering occurs at the surface of sample. Outer atom bonding conceivably weaker than inner bonding. That is, the energy of sputtering is lower than the energy of atomic displacement. If the specimens are thick enough, the problem of sputtering can be negligible because properties of specimen aren't change much by any loss atoms on the surface. To avoid damage of electron sputtering is to reduce electron dose or cover a thin layer of a heavy element.

1.1.5.3 Electrostatic charging

Charging of electrically insulated specimen has two way, one is elastic scattering (backscattered electrons) and the other is inelastic scattering (secondary electrons). Secondary electrons signals are considered only in Scanning Electron Microscopy (SEM). But now these signal also used in Scanning Transmission Electron Microscopy (STEM) to form higher resolution topography images than SEM.

There are two types of secondary electrons, which in specimen ejected by incident beam. One is the electrons having energies <50 eV are in conduction or valence band and the other is the electrons called Auger electrons ejected from inner shell when an ionized atom returns to its ground state. Because secondary electrons are weak so that they only can be ejected from the surface of specimen, forming images in SEM. This damage can cause a mechanical force on a sample. [5]

1.1.6 Paradox

Radiolysis is reduced at higher voltage while knock-on damage is increased. So the damage depend on the voltage, we need to take this paradox into account before the TEM experiments.

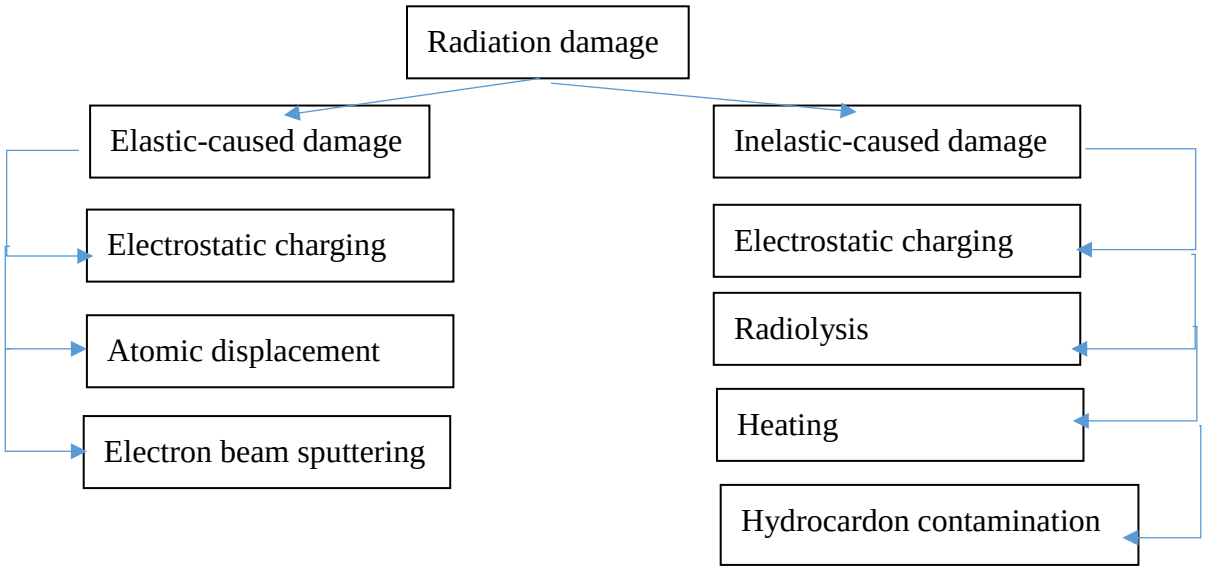

Figure 2. Types of radiation damage

1.2 Metal organic frameworks

Recently, climate change has been increasingly observable on the earth. Carbon dioxide (CO_2) has been blame for primary cause of changes. [6] The rise of temperature and sea level, species extinction, shifting crop harvest and so on are too crucial to cause greenhouse gas CO_2 got human attention. Carbon capture and storage (CCS) is one of promising approaches to subside those calamity. Several technologies including cryogenic distillation, chemical absorption and physical adsorption have been applied. Metal Organic Frameworks (MOF), one of physical adsorption, have attracted much interests in last two decades due to their high surface area and low density. [7] Recently, alkali-metal ions doped MOFs have been found significantly

increasing the CO2 adsorption. Lithium-doped MOFs have greater CO_2 adsorption than another alkali-metal doped MOFs. [8] Several reports also show that synthesizing open metal sites containing MOFs have higher CO_2 adsorption. [9] Other than synthesizing open metal sites, post-synthetic approaches are also suitable for MOFs. [10]

1.2.1 Synthesis of MOFs

Within past decades, development of synthetic methods to control particle size and shape has increased exponentially. Upon those methods, there are parameters that affect MOF structure such as nature of solvent, temperature and metal precursor. Nature of solvent controls solubility of reagents, thus it indirectly controls the shape of final particles and particle size. [11] Recent report shows that higher temperature factors in kinetic of crystal formation, thus resulting larger particles. [12] Using of metal precursor has critical impact on MOFs crystal shape and proportions. [13]

1.2.1.1 Direct precipitation

This synthesize method is the most common methods for MOFs. The method is directly mixing liquid with metal ions and bridging ligands. Auto-assembly occurs

when supersaturation, a state of solution containing more of the dissolved material than solvent can dissolved in normal condition, has reached. Direct precipitation can control the size and morphology by revising reaction process.

1.2.1.2 Conventional heating methods

This methods transfer thermal energy from heating source to mixed solution. Thermal energy is generated by friction of dipole rotation. Also, there are different parameters makes researcher harder to control particle shape and morphology influenced by gradients of concentration and temperature of reaction.

1.2.1.3 Microwave and ultrasound driven synthesis

Different from heating methods, dipole rotation and ionic conduction are primary ways to transfer energy. This method only influences the molecules with dipole or being ionic. The energy is generated by collisions of charged particles, making energy transferring more efficient due to energy is transferred to mixing solution not to the vessel.

1.2.1.4 Electrochemical synthesis

Electrochemical synthesis provides better control of crystal growth than

conventional synthesis. This method also been used for thin film growth on electrodes that act as metal source.

1.2.1.5 Presence of ionic liquids (IL)

Ionic liquids (IL), a good solvent for various organic or inorganic compounds, is the latest promising media for MOFs synthesis. As a report show that changing the length of n-alkyl chain on 1-R-3-methylimidazolium tetrafluoroborate [RMIM] [BF_4] IL cation can control different sizes of generated particles. [14]

Chapter 2

Experiment and Analysis

2.1 Radiation damage study of metal organic frameworks (MOFs)

2.1.1 Dose test

Following figure 3 presents a set of before-after radiation damage on NiCu MOF. The beam damage (dark points) increasing in size with time increasing after bombardment with 200keV electrons.

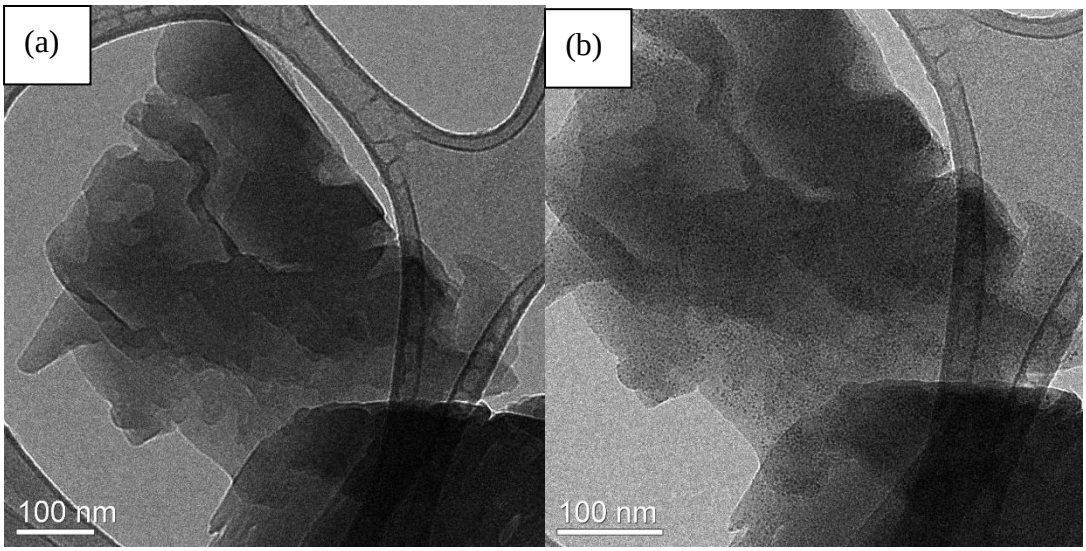

Figure 3. Before-after radiation damage of NiCu MOF (a) before damaged (b) after damaged

2.1.2 Procedure of dose test

To use selected area electron diffraction to acquire undistorted and symmetric diffraction patterns, following steps are required:

1. Choose the high tilt holder, which is suitable for sensitive samples and which can

tilt over 25 degrees compared with single tilt holder.

2. Follow fundamental steps of JEOL 1400 (120keV).
3. Choose an area that could have only one grain and insert selected area aperture to make electrons only illuminated the area we want.
4. Take one image in image mode (Figure 4 (a)) and ensure that there are bright area making use of calculating dose rate.
5. Transfer to diffraction mode and acquire one image (Figure 4 (b)).
6. Keep tracking on the diffraction image every period of time until all reflections are disappeared.
7. Repeat (1) to (6) to have few sets for statistical analysis.

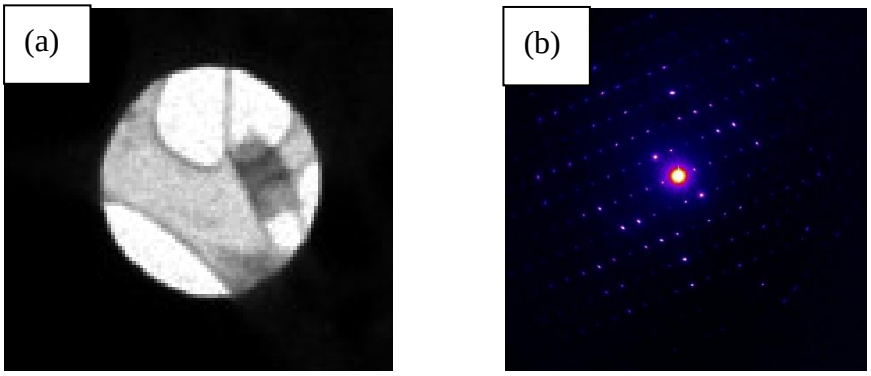

Figure 4. Selected area electron diffraction pattern of NiCo MOFs (a) The area we chose has only one grain at magnification of 1200 KX (b) Single diffraction pattern of the selected area

2.1.3 Procedure of analysis

After acquiring sets of diffraction images, the next step is to analyze these:

1. Use ROI tool in DigitalMicrograph to know the mean electron counts and also exposure time and area can be found in image display Info.
2. Calculate the dose rate (DR), using the following formula.

DR = $\frac{mean\ (e^-)}{exposure\ time\ (s) * area\ (Å^2)}$ $(\frac{e^-}{s * Å^2})$

3. Choose four reflections and measure their k-value (1/nm) respectively.
4. Open Image J software.
5. Import a set of diffraction images to make a series of images.
6. Use a plugin called template matching to align images and the matching method is normalized correlation coefficient.
7. After alignment, use ROI manager in analyze and apply a rectangle to fit with the four reflections we chose in previous steps.
8. Measure all mean intensities in each reflections of each diffraction images.
9. Attain electron dose (D) by multiplying a period of time, using following formula.
10. D = Time * DR $(\frac{e^-}{Å^2})$
11. Import all calculated data into Origin software and obtain a plot between intensity and electron dose (D)
12. Fit the plot by exponential because critical dose is the dose where intensity decline to $\frac{1}{e}$, the formula can be present in this way

    I = A + B Exp($\frac{D}{D_e}$) where D_e is the critical dose

    So that we can attain critical dose from reciprocal of D's parameter.

2.2 Analysis of MOFs

2.2.1 Analysis of Cu metal organic framework (MOF)

The figure is the diffraction pattern of Cu MOF, although this pattern is more likely to

be polycrystalline, analysis is still valid. Four reflections has been chosen.

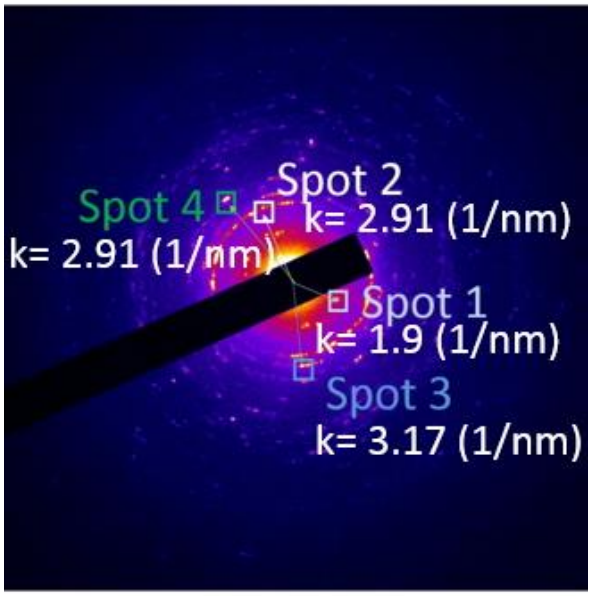

Figure 5. Reflections chosen from Cu MOF diffraction pattern

The dose rate (DR) we measure from image is 0.037 ($\frac{e^-}{S* Å^2}$) and then start illuminating the area.

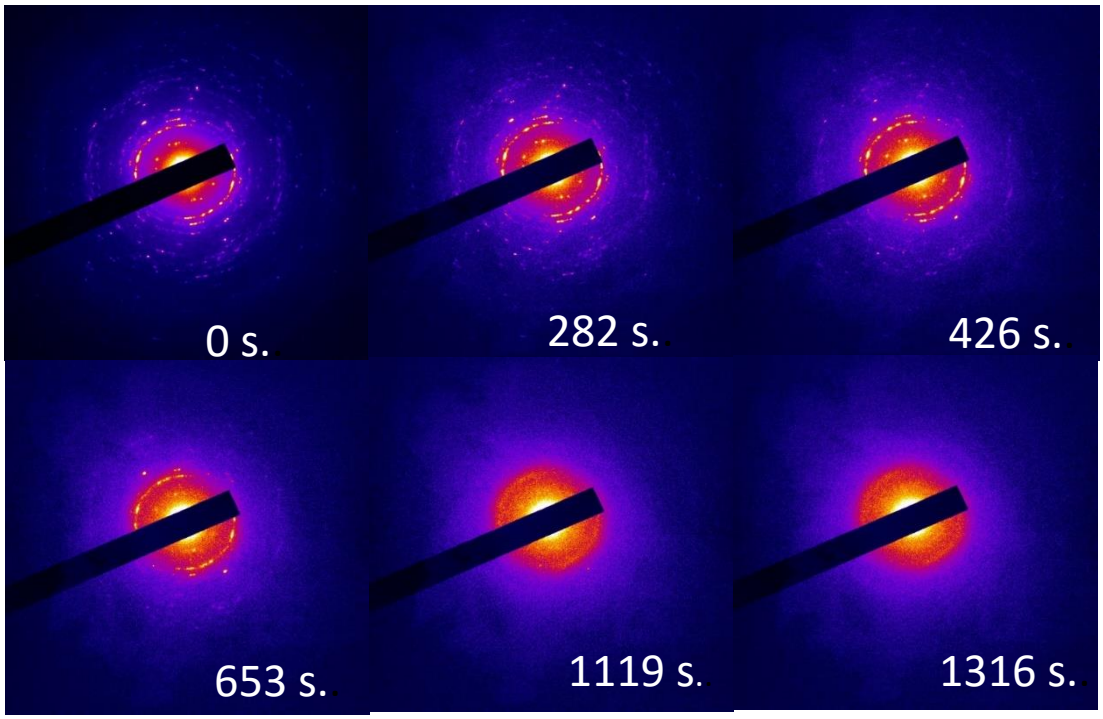

Figure 6. Time series of dose test of Cu MOF

Best fit the intensity-dose with exponential to get critical dose respectively.

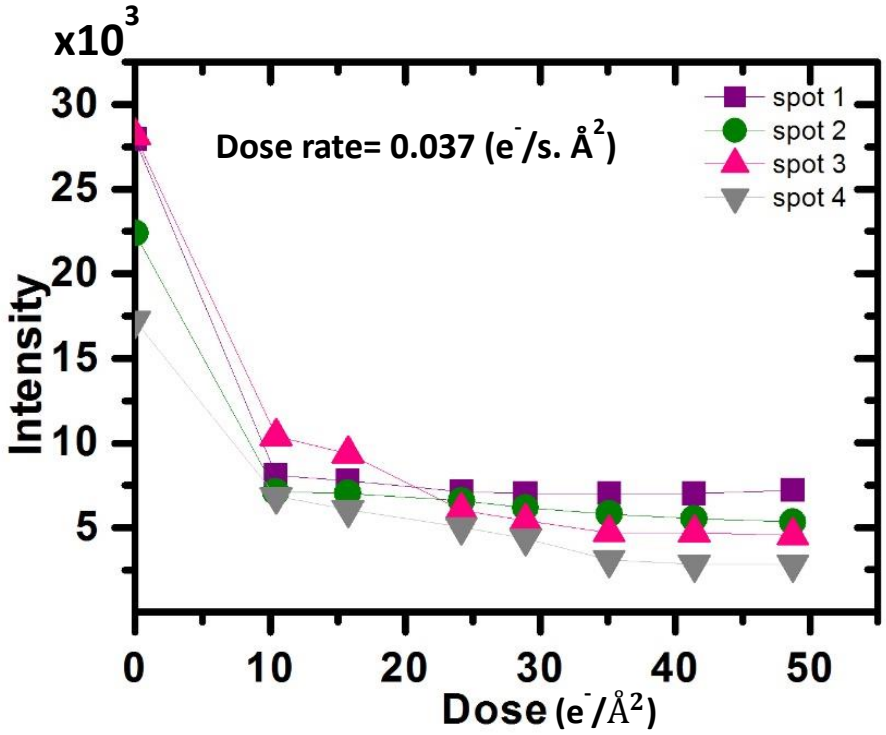

Figure 7. Intensity-Dose of Cu MOF

And then we compared critical dose of four reflections.

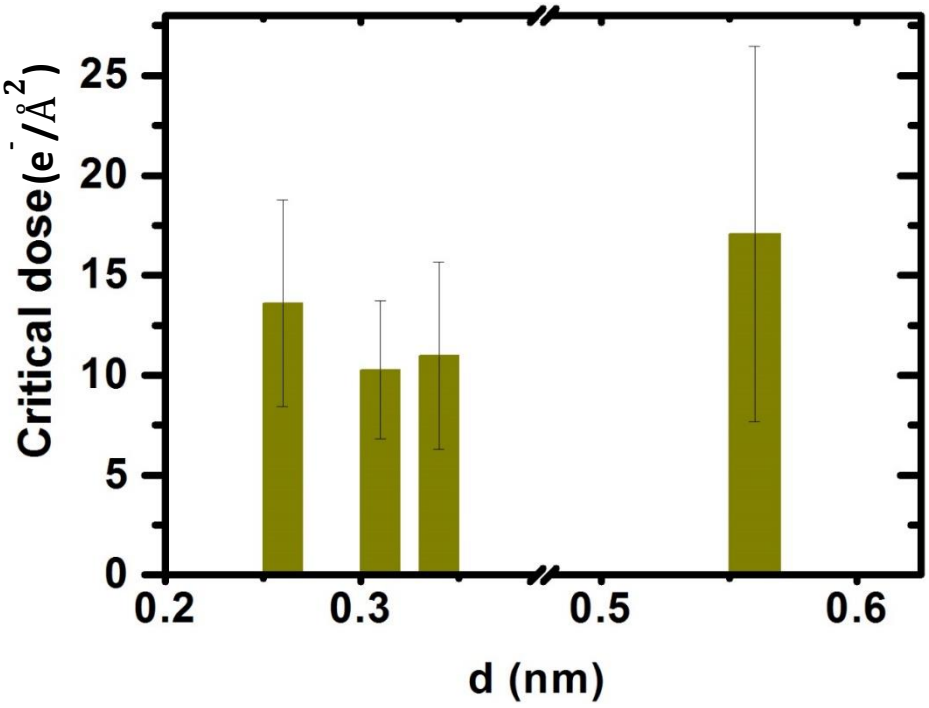

Figure 8. Critical dose of Cu MOF

d (nm)	Critical dose ($\frac{e^-}{Å^2}$)
0.56	17.07
0.34	10.98
0.31	10.27
0.26	13.6

Table 1. Spacing of Cu MOF against critical dose respectively

2.2.2 Analysis of Ni metal organic framework (MOF)

The figure is the diffraction pattern of Ni MOF. Four reflections have been selected as followed.

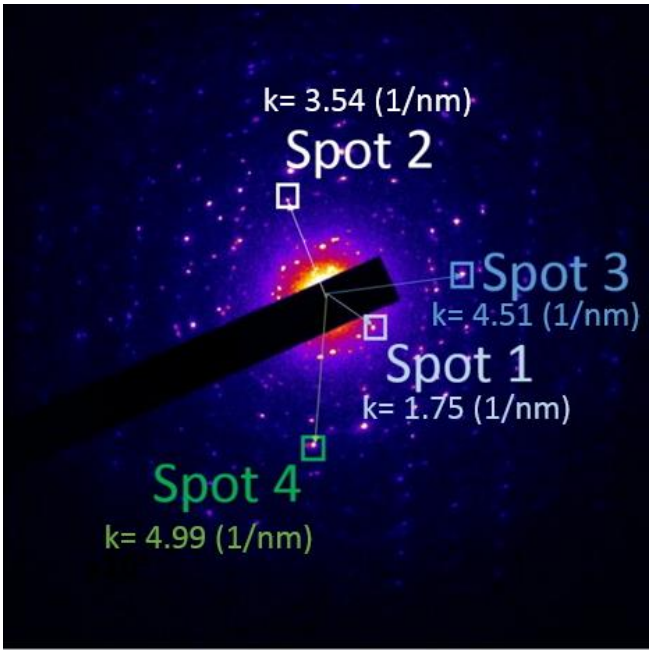

Figure 9. Reflections chosen from Ni MOF diffraction pattern

The dose rate (DR) we measure from image is 0.51 ($\frac{e^-}{s* Å^2}$) and then start illuminating the area.

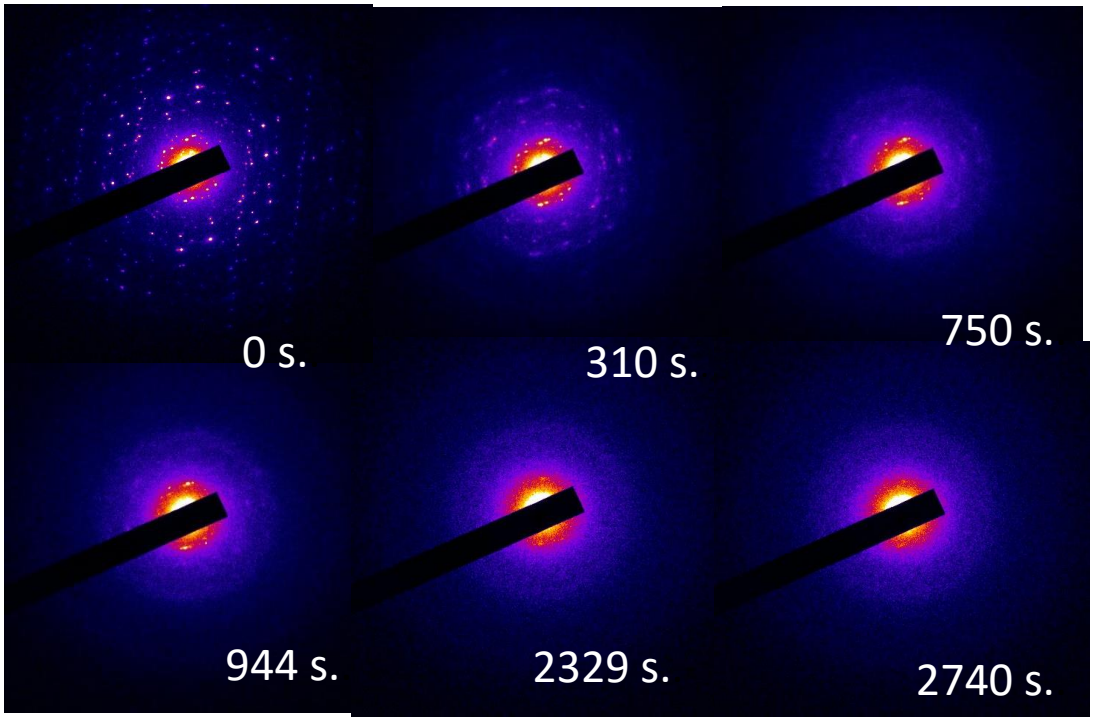

Figure 10. Time series of dose test of Ni MOF

Best fit the intensity-dose with exponential to get critical dose respectively.

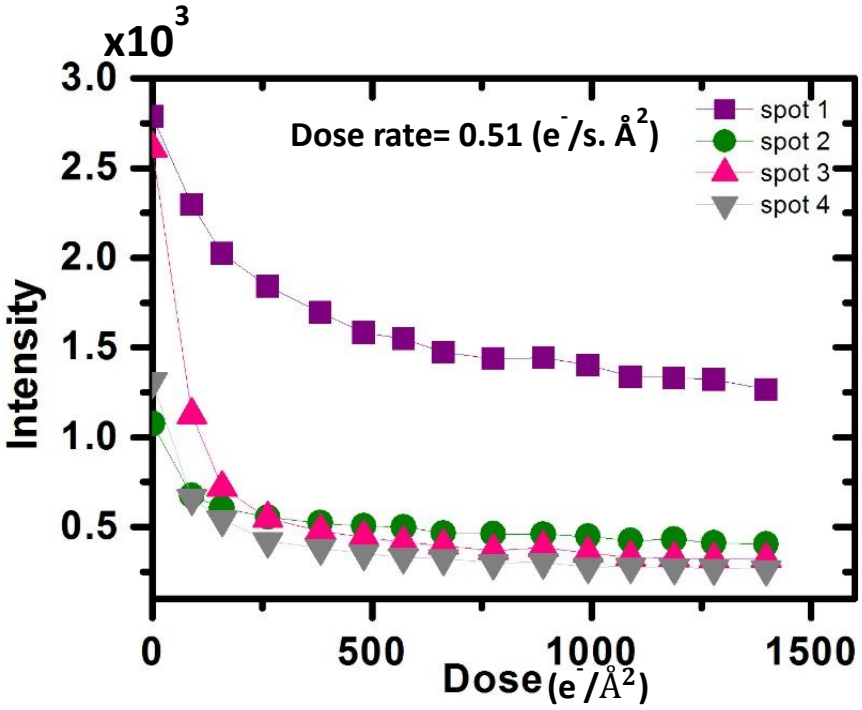

Figure 11. Intensity-Dose of Ni MOF

And then we compared critical dose of four reflections.

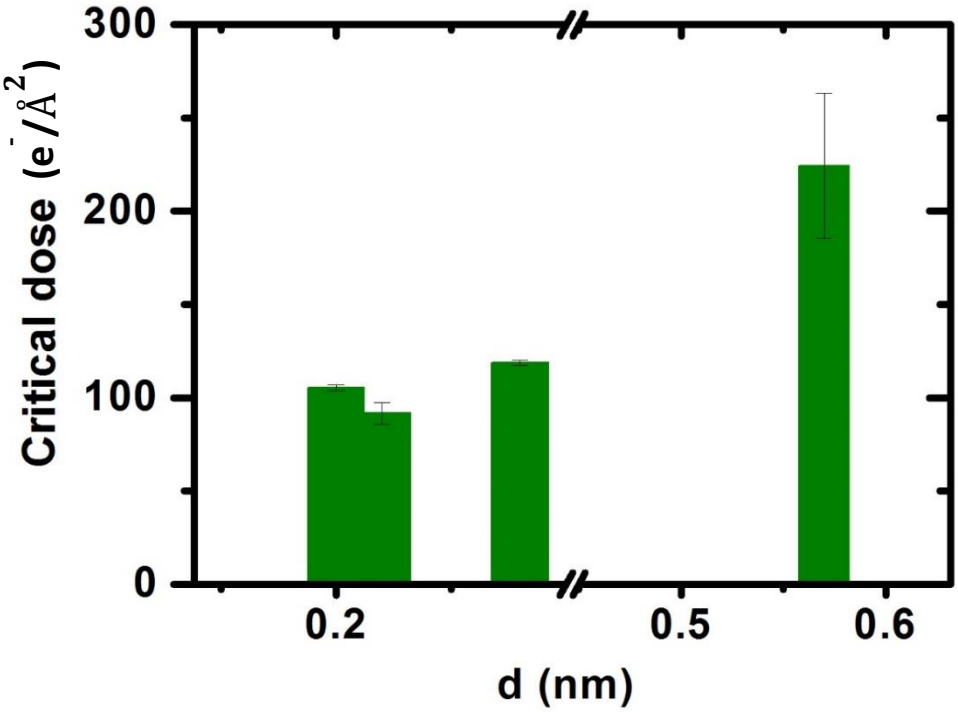

Figure 12. Critical dose of Ni MOF

d (nm)	Critical dose ($\frac{e^-}{Å^2}$)
0.57	224.33
0.28	118.77
0.22	91.65
0.2	105.32

Table 2. Spacing of Ni MOF against critical dose respectively

2.2.3 Analysis of NiCu metal organic framework (MOF)

The figure is the diffraction pattern of NiCu MOF. Four reflections have been selected as followed.

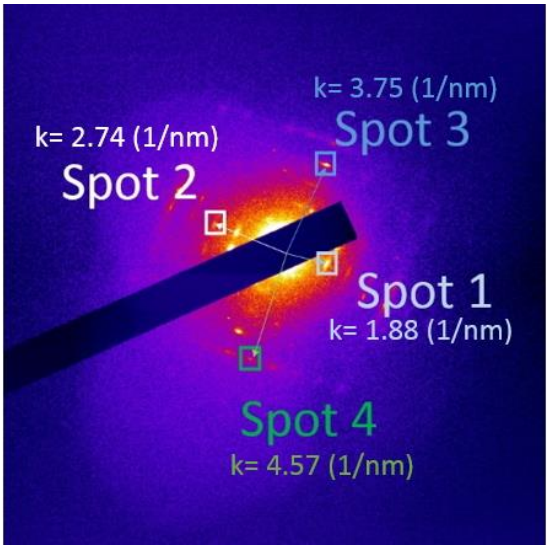

Figure 13. Reflections chosen from NiCu MOF diffraction pattern

The dose rate (DR) we measure from image is 1.029 ($\frac{e^-}{s* Å^2}$) and then start illuminating the area.

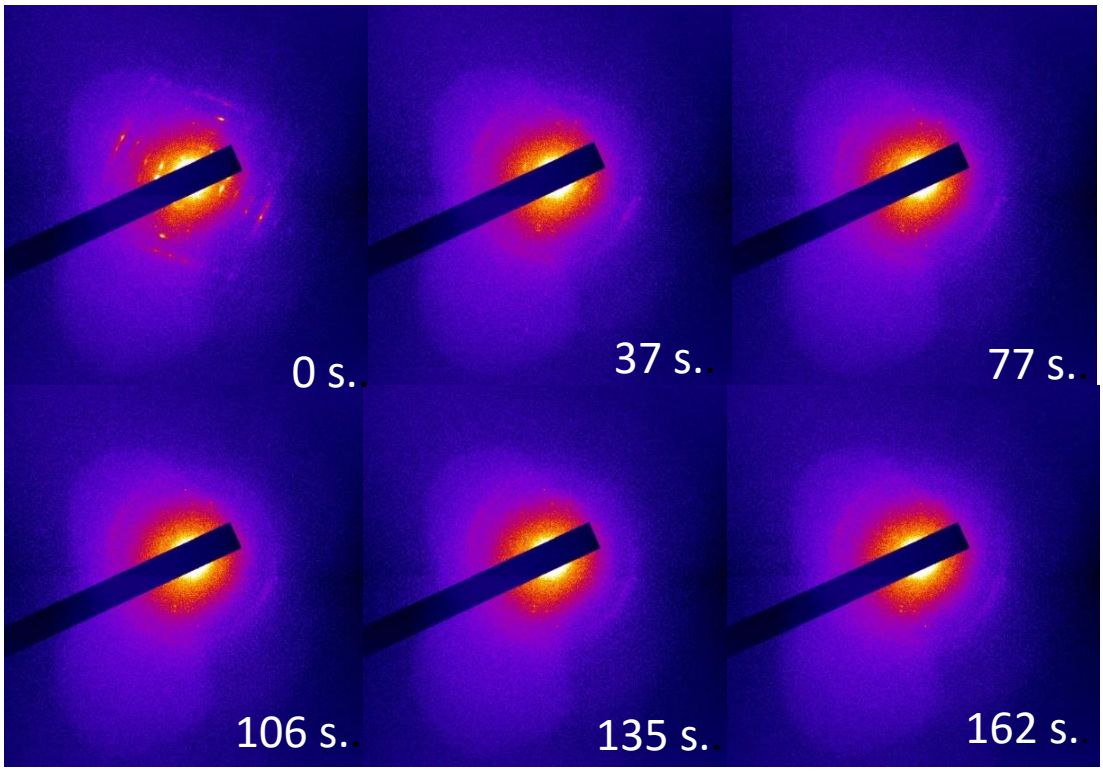

Figure 14. Time series of dose test of NiCu MOF

Best fit the intensity-dose with exponential to get critical dose respectively.

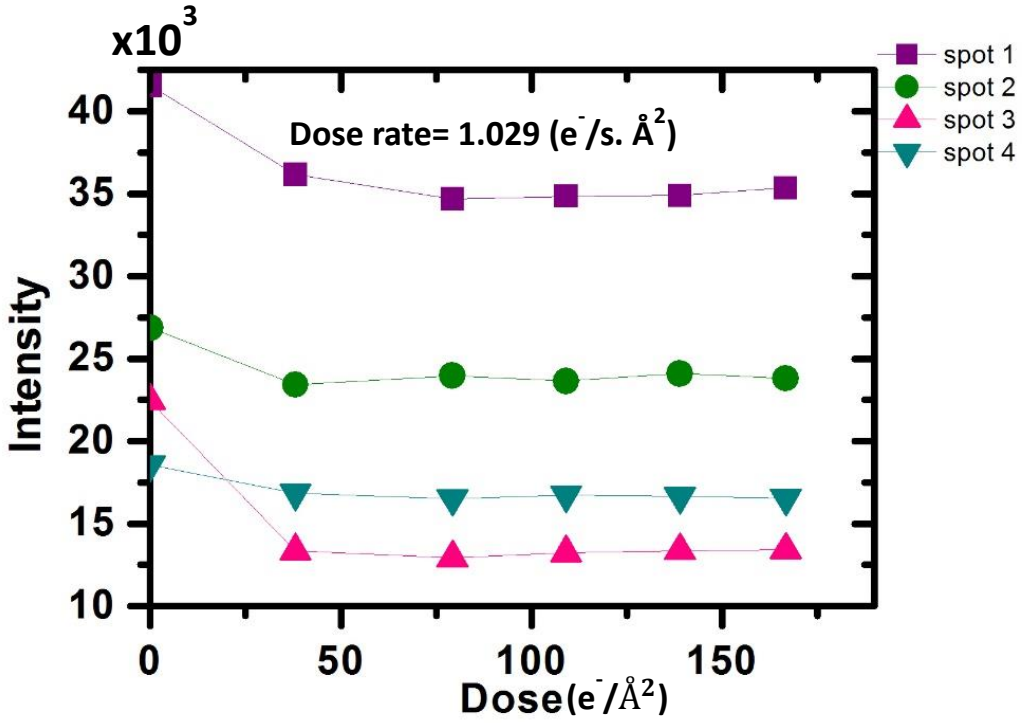

Figure 15. Intensity-Dose of NiCu MOF

And then we compared critical dose of four reflections.

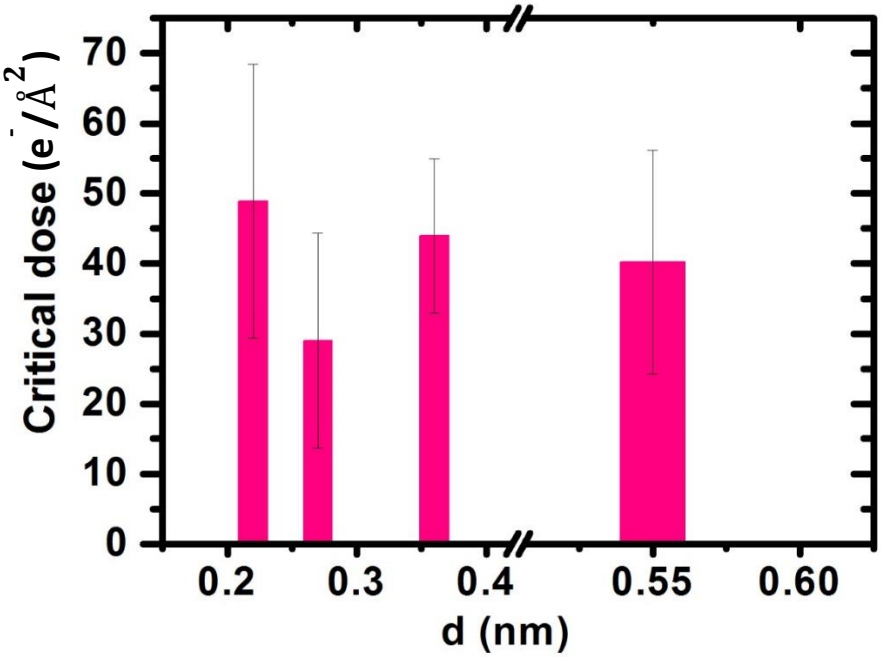

Figure 16. Critical dose of NiCu MOF

d (nm)	Critical dose ($\frac{e^-}{Å^2}$)
0.55	40.22
0.36	43.94
0.27	29
0.22	48.88

Table 3. Spacing of NiCu MOF against critical dose respectively

2.2.4 Analysis of NiCo metal organic framework (MOF)

The figure is the diffraction pattern of NiCo MOF. Four reflections have been selected as followed.

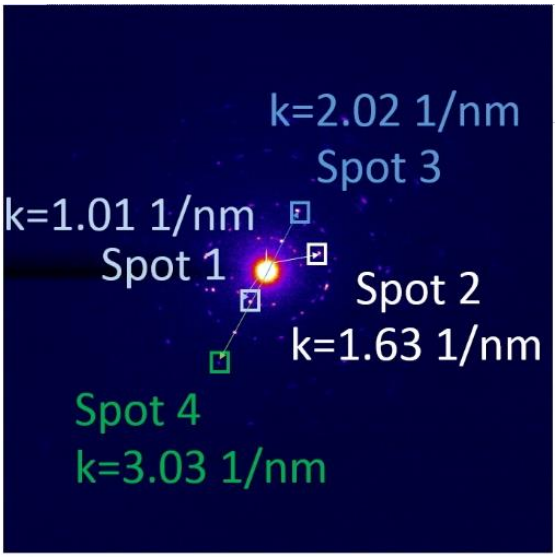

Figure 17. Reflections chosen from NiCo MOF diffraction pattern

The dose rate (DR) we measure from image is 0.39 ($\frac{e^-}{s* Å^2}$) and then start illuminating the area.

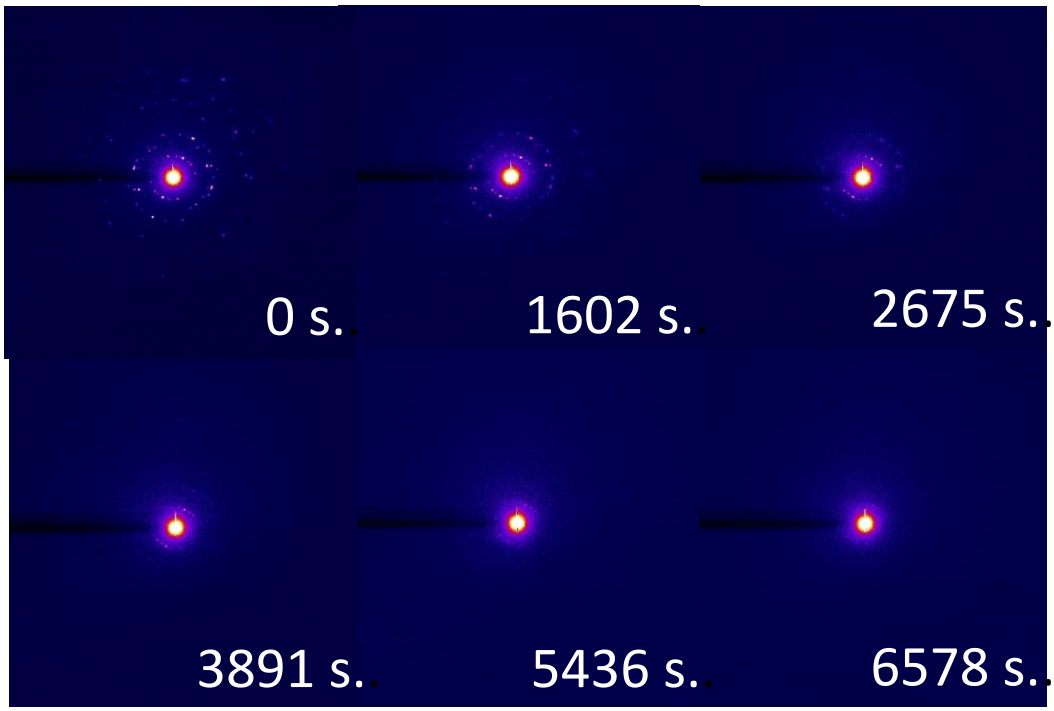

Figure 18. Time series of dose test of NiCo MOF

Best fit the intensity-dose with exponential to get critical dose respectively.

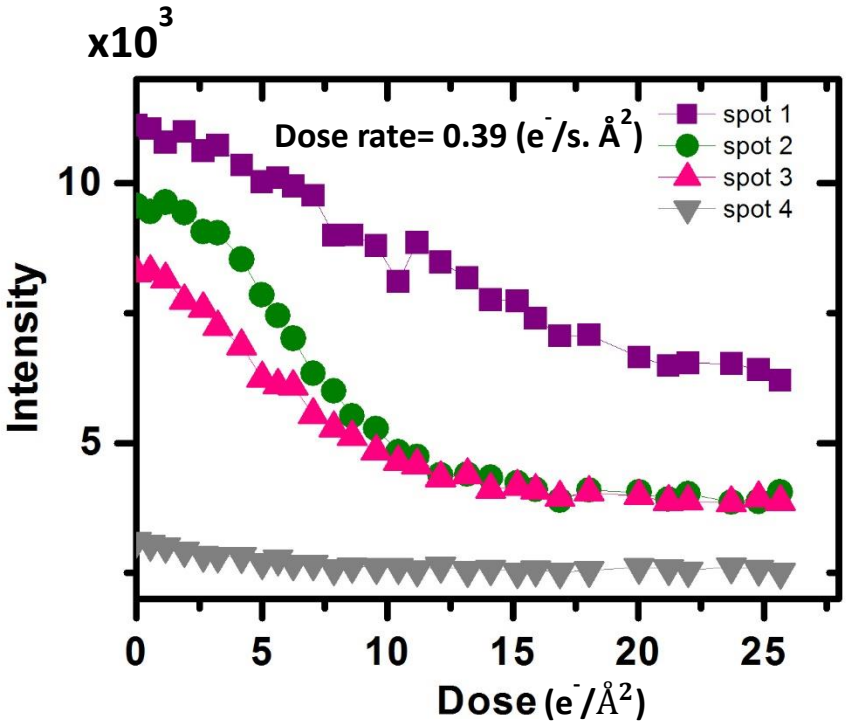

Figure 19. Intensity-Dose of NiCo MOF

And then we compared critical dose of four reflections.

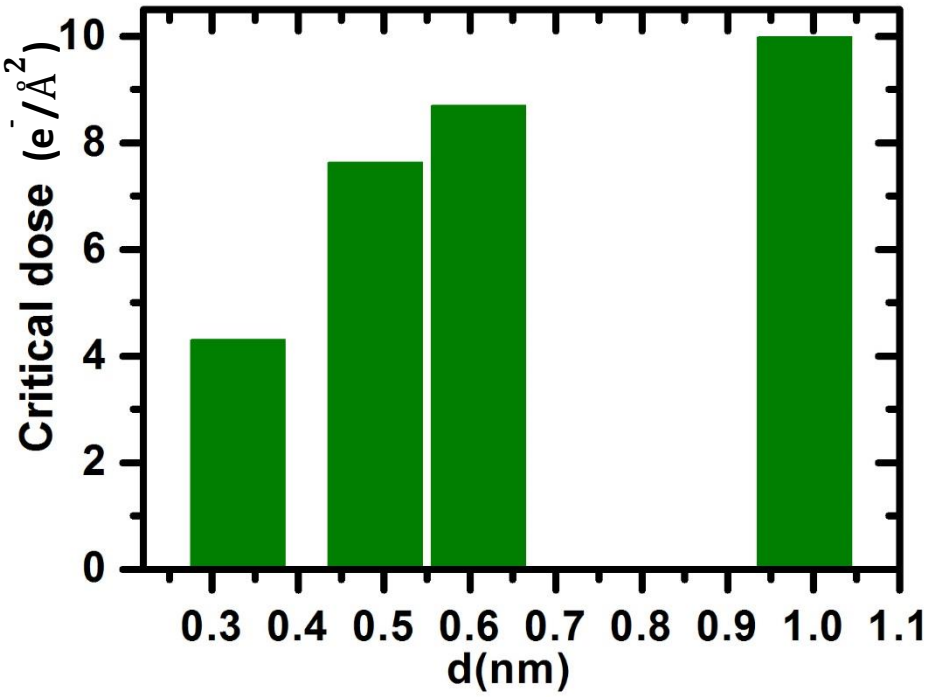

Figure 20. Critical dose of NiCo MOF

d (nm)	Critical dose ($\frac{e^-}{Å^2}$)
0.55	40.22
0.36	43.94
0.27	29
0.22	48.88

Table 4. Spacing of NiCo MOF against critical dose respectively

2.2.5 Analysis of CoCu metal organic framework (MOF)

The figure is the diffraction pattern of CoCu MOF. Four reflections have been selected as followed.

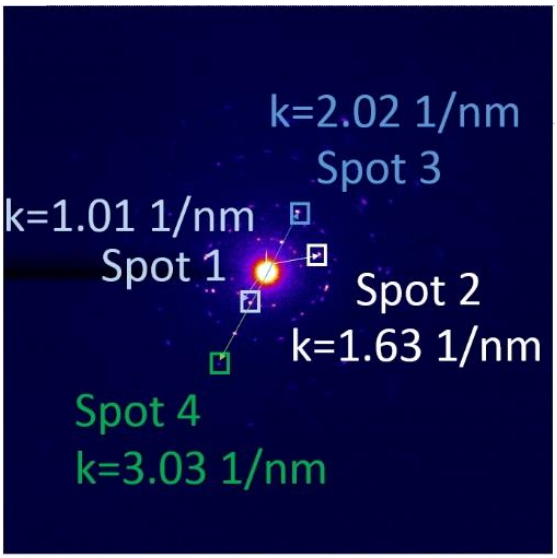

Figure 21. Reflections chosen from Cu MOF diffraction pattern

The dose rate (DR) we measure from image is 0.024 ($\frac{e^-}{s* Å^2}$) and then start illuminating the area.

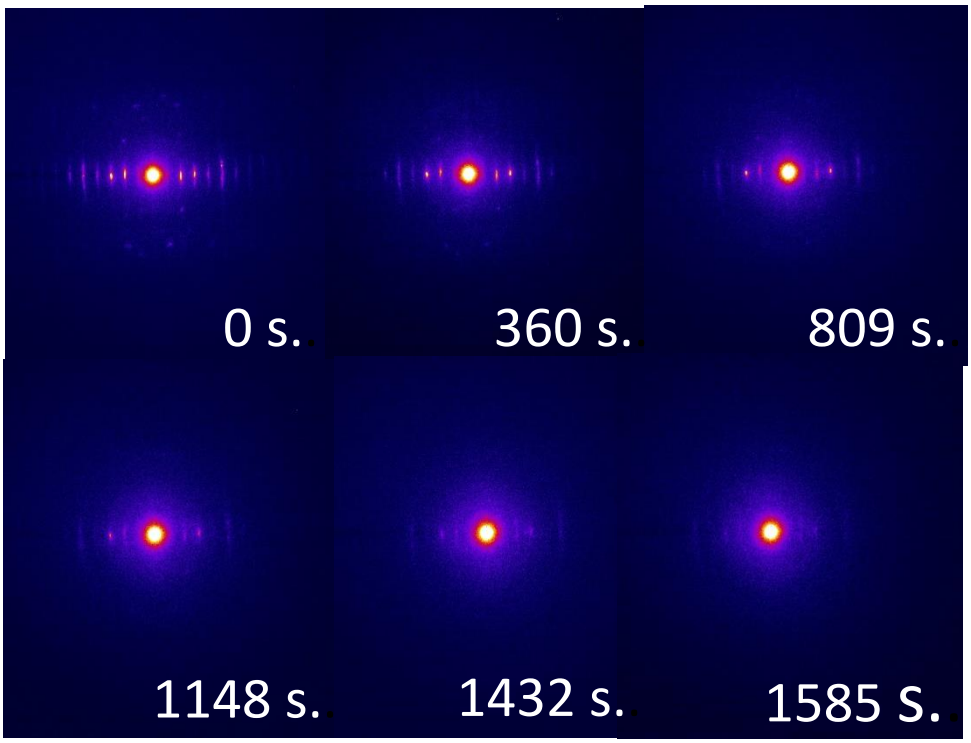

Figure 22. Time series of dose test of CoCu MOF

Best fit the intensity-dose with exponential to get critical dose respectively.

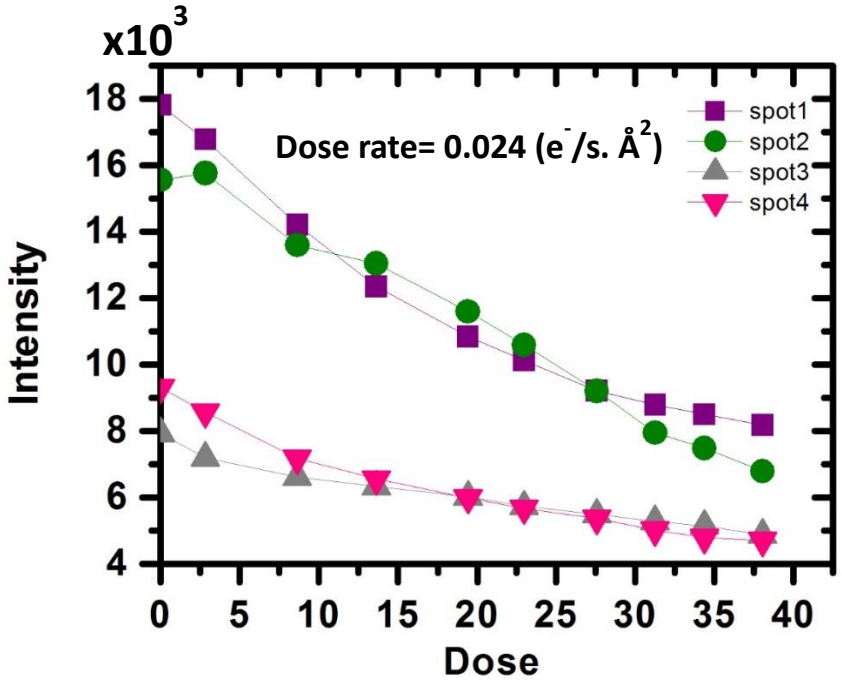

Figure 23. Intensity-Dose of CoCu MOF

And then we compared critical dose of four reflections.

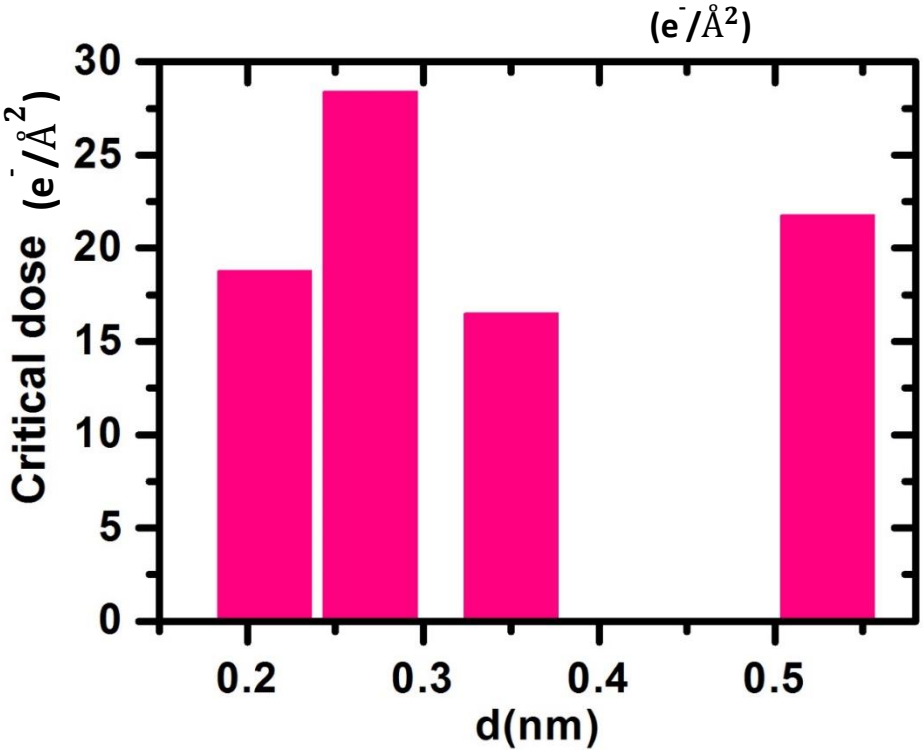

Figure 24. Critical dose of CoCu MOF

d (nm)	Critical dose ($\frac{e^-}{Å^2}$)
0.53	21.77
0.35	16.52
0.27	28.41
0.22	18.79

Table 5. Spacing of CoCu MOF against critical dose respectively

2.2.6 Analysis of NiCoCu metal organic framework (MOF)

The figure is the diffraction pattern of NiCoCu MOF. Four reflections have been selected as followed.

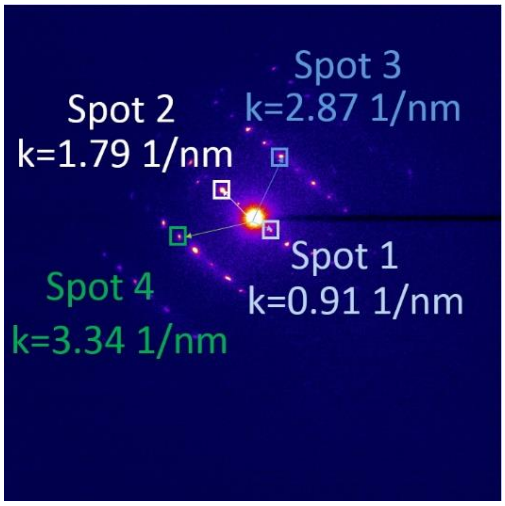

Figure 25. Reflections chosen from NiCoCu MOF diffraction pattern

The dose rate (DR) we measure from image is 0.013 ($\frac{e^-}{s* Å^2}$) and then start illuminating the area.

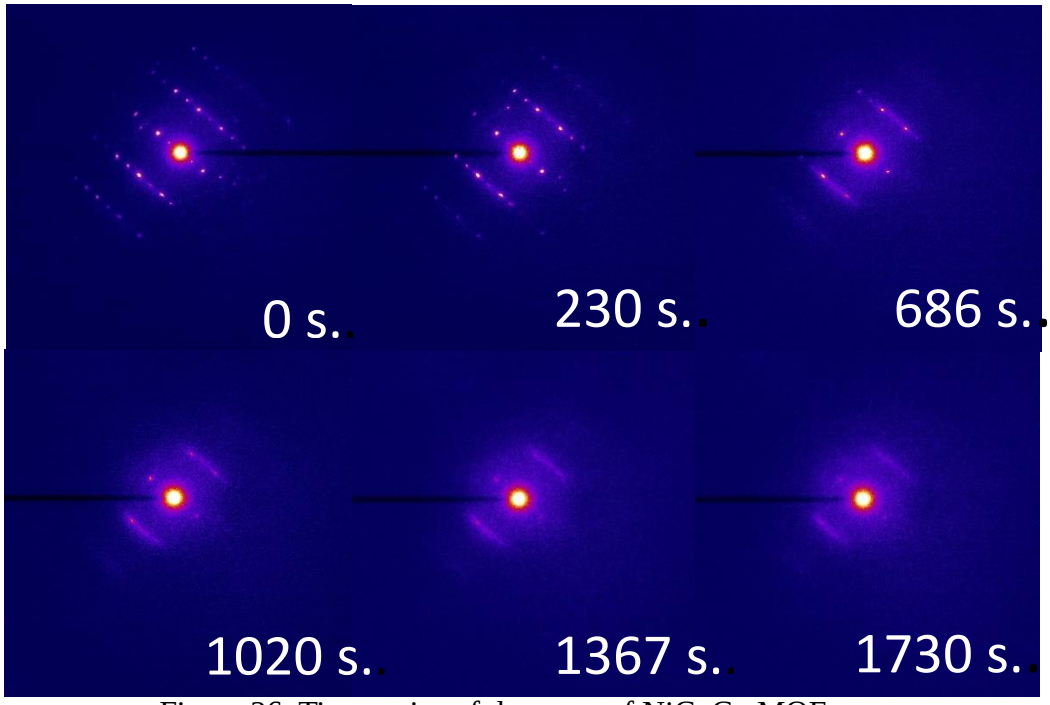

Figure 26. Time series of dose test of NiCoCu MOF

Best fit the intensity-dose with exponential to get critical dose respectively.

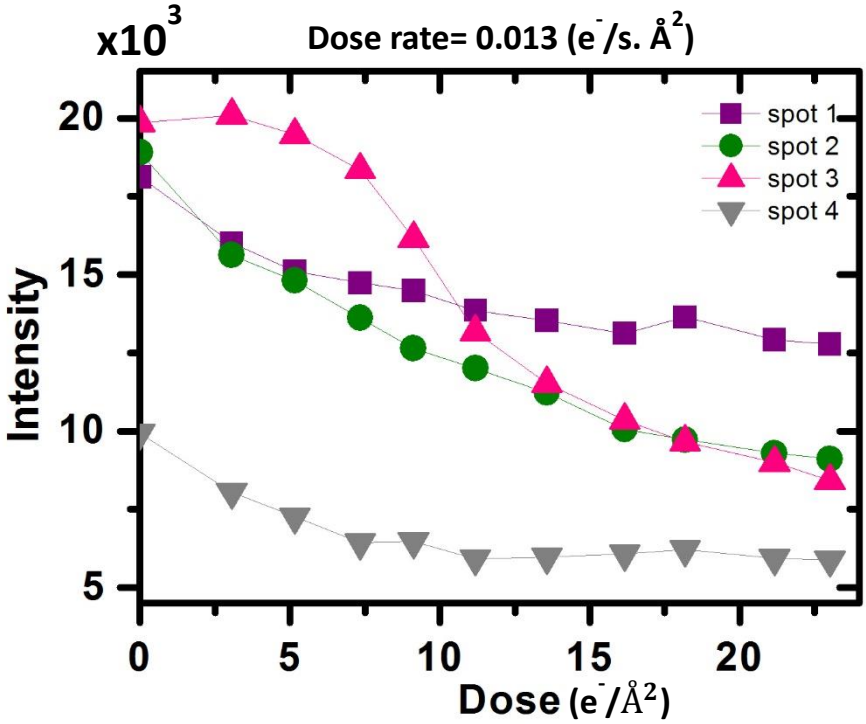

Figure 27. Intensity-Dose of NiCoCu MOF

And then we compared critical dose of four reflections.

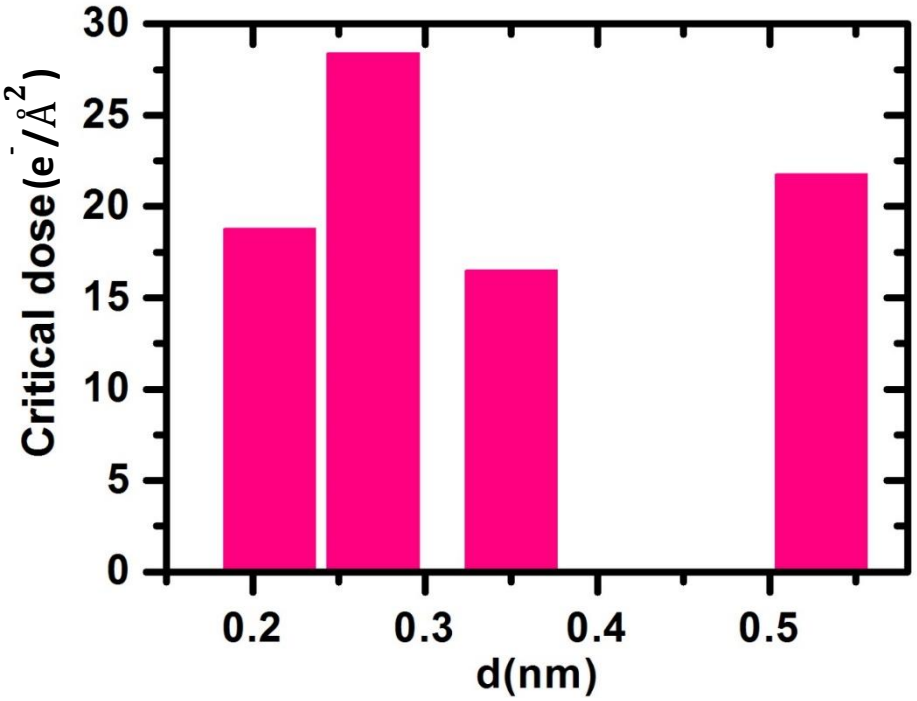

Figure 28. Critical dose of NiCoCu MOF

d (nm)	Critical dose ($\frac{e^-}{Å^2}$)
1.1	7.41
0.55	12.25
0.35	16.98
0.285	7.59

Table 6. Spacing of NiCoCu MOF against critical dose respectively

Chapter 3

Conclusion

3.1 Dose rate in each spot size

Before doing dose test, approximately calculating dose rate in every spot size help the research process going smoothly. Here is the table applied in magnification 200K, which is proper dose rate for polymer DPP.

Spot size	Dose rate
2	$1.18*10^{-2}$
3	$1.67*10^{-3}$
4	$5.89*10^{-4}$
5	$4.1*10^{-5}$

Table 7. Dose rate when magnification is 200K

As the table shows, dose rate is increasing when spot size decreases. Dose rate at spot size 4 is 14 times of dose rate at spot size 5. Also, Dose rate at spot size 3 is 2.8 times of dose rate at spot size 4. Dose test is suitable at spot size 3 and tilt series is suitable at spot size 4.

Again, we measure the dose rate at magnification 1200K to see whether dose rate is magnification-dependent or not.

Spot size	Dose rate
2	0.053
3	$8.69*10^{-3}$
4	$2.32*10^{-3}$
5	$1.65*10^{-4}$

Table 8. Dose rate when magnification is 1200K

The table shows that dose rate at spot size 4 is 14 times of dose rate at spot size 5. Also, Dose rate at spot size 3 is 3 times of dose rate at spot size 4. The result of 1200K is similar to of 200K, then we conclude that the dose rate is magnification-independent but only spot-size-dependent. That is, this could be a method preventing radiation damage after being informed the dose rate at each spot size in certain magnification.

3.2 Systematized dose test of MOFs samples

In order to optimize the research on MOFs samples and avoid radiation damage of electron beam, persisting calculating dose rate is necessary. As the table below recommended the dose rate used during dose test on each MOF samples. But experiments except dose test should always below these values to prevent electron beam damage.

MOF sample name	Dose rate ($\frac{e^-}{s* Å^2}$)	Duration time (seconds)
Cu	0.37	1316
Ni	0.51	2740
NiCu	0.041	1193
NiCo	0.39	6578
CoCu	0.024	1585
NiCoCu	0.013	1730

Table 9. Recommended dose rate used in dose test and approximate duration time

The ideal duration time of dose test is around 20 minutes (1200 seconds) because this could not only save time but also reduce burden of analysis. For NiCo, the duration time is around 2 hour therefore analysis becomes hard work. If we acquire image every 3 minutes, the total number of images will be 40.

3.3 Summarization of MOFs dose test

Following figure and table are comparison of each MOF sample.

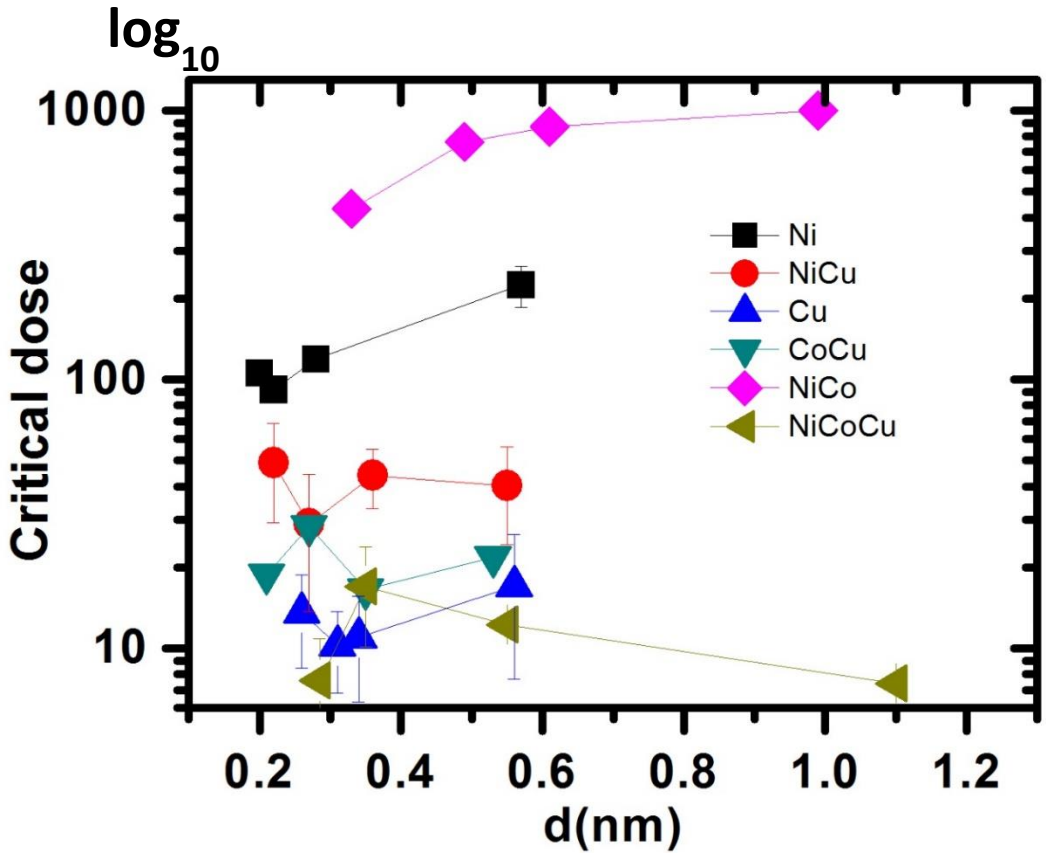

Figure 29. Critical dose against spacing of each MOF sample

Sample name	Max critical dose	Spacing (nm)	Spacing of strongest reflection	The largest spacing (nm)
Cu	17.07	0.56	0.56	0.56
Ni	224.33	0.57	0.57	0.57
NiCu	48.88	0.22	0.55	0.55
NiCo	999.18	0.99	0.99	0.99
CoCu	28.41	0.27	0.53	0.53
NiCoCu	16.98	0.35	0.35	1.1

Table 10. Comparison of each MOF sample

Comparatively, NiCo MOF has the highest critical dose and NiCoCu MOF has the lowest. During experiments, we discovered that dose rate is independent of critical dose. Also, the MOF that has nickel (Ni) stabilized structure during radiation of electron beam. However, the MOF that has copper (Cu) made structure less stable and copper has priority when determine the crystal is stable or not. That is to say, if MOFs have copper, the structure will be less stable regardless containing nickel.

According to Table 10, the maximum critical dose (D_e) is not always be the largest spacing, reflections. Also, the largest spacing doesn't always present the strongest intensity reflection.

Reference

[1] Xiadong Zou, Sven Houvmoller, Peter Oleynikov, Electron Crystallography, (2011) 84-88

[2] David B. Walliams, C. Barry Carter, Transmission Electron Microscopy, second edition, (2009) 27-28

[3] David B. Walliams, C. Barry Carter, Transmission Electron Microscopy, second edition, (2009) 64-68

[4] Shuaxue Jin, Liping Guo, Yaoyao Ren, Rui Tang, Yanxin Qiao, TEM characterization of self-ion irradiation damage in Nickel-base alloy C-276 at elevated temperature, J. Master. Sci. Technol., 2012, 28(11) 1039-1045

[5] R.F. Egerton, P. Li, M. Malac, Radiation damage in the TEM and SEM, Micron 35 (2004) 399-409

[6] Z. Chen, S. Deng, H. Wei, B. Wang, J. Huang, G. Yu, Polyethlenimine-impregnated resin for high CO_2 adsorption: an effect absorbent for CO2 capture from simulated flue gas and ambient air, ACS Appl. Mater. Interface 5 (2013) 6937-6945

[7] T.C. Wang, W. Bury, D.A. Gomes-Gualdron, N.A. Vermeulen, J.E. Mondloch, P. Deria, K. Zhang, P.Z. Moghadam, A.A. Sarjeant, R.Q. Snurr, J.F. Stoddart, J.T. Hupp, O.K. Farha, Ultrahigh surface area zirconium MOFs and insights into applicability of the BET theory, J. Am. Chem. Soc. 137 (2015) 683-690

[8] J. Lan, D. Cao, W. Wang, B. Smit, Doping of alkali, alkaline-earth, and transition metals in covalent-organic frameworks for enhancing CO_2 capture by first principles calculations and molecular simulations, ACS Nano 4 (2010) 4225-4237

[9] J. Kan, D. Cao, W. Wang, B. Smite, Doping of alkali, alkaline-earth and transition metals in covalent-organic frameworks for enhancing CO_2 capture by first principles

calculations and molecular simulations, ACS Nano 4 (2010) 4225-4237

[10] X. Yan, S.Komarneni, Z. Zhang, Z. Yan, Extremely enhanced CO_2 uptake by HKUST-1 metal organic framework via a simple chemical treatment, Microporous Mesoporous Mater. 183 (2014) 69-73

[11] S. Jung, M.Oh, Angew, Monitoring shape transformation nanocubes and size-controlled for coordination polymer particles, Chem. Int. Ed. Engl. 47 (2008) 2049-2051

[12] A. Demessence, D.M. D'Alessandro, M.L. Foo, J.R. Long, Strong CO_2 binding in a water-stable, triazolate-bridged metal-organic framework functionalized with ethylenediamine J. Am. Chem. Soc. 131 (2009) 10662-10669

[13] Beatriz Seoane, Sonia Castellanos, Alla Dikhtiarenko, Freek Kapteijn, Jorge Gascon, Multi-scale crystal engineering of metal organic frameworks, Coodination Chem. Review 307 (2016) 147-187

[14] G.Clavel, J. Larionova, Y. Guari, C. Guerin, Synthetic of Cyano-Bridged magnetic nanoparticles using room-temperature ionic liquids, Chem. Eur. J. 12 (2006)3798-3804